Auxetic interpenetrating composites: A new approach to non-porous materials with a negative or zero Poisson's ratio

Zhengyang Zhang[1], Hanxing Zhu[1*], Ru Yuan[2], Sanmin Wang[2], Tongxiang Fan[3], Yacine Rezgui[1], Di Zhang[3]

[1] School of Engineering, Cardiff University, Cardiff CF24 3AA, UK

[2] School of Mechanical Engineering, Northwestern Polytechnical University, Xi'an 710072, China

[3] State Key Lab of Metal Matrix Composites, School of Materials Science and Engineering, Shanghai Jiao Tong University, Shanghai 200240, P.R. China

[*]e-mail: zhuh3@cardiff.ac.uk

Abstract

In this research, the Poisson's ratio of three different types of almost isotropic interpenetrating composites are designed to be either positive, or negative, or zero. As they are strengthened by a self-connected fibre-network and do not contain any pore in their structure, they all are stiffer than the conventional particle composites. In addition, structural hierarchy is also demonstrated to be able to significantly enhance the auxetic behaviour for the three types of interpenetrating composites. Thus, these composites could be used not only as functional materials, but also as structural materials in engineering applications.

Keywords: Auxetic behaviour; negative Poisson's ratio; interpenetrating composite; Structural hierarchy.

1. Introduction

The classical theory of elasticity [1,2] shows that the Poisson's ratio of an isotropic material could be in the range of $-1 < \nu < 0.5$. However, most non-porous natural and engineered isotropic materials exhibit a positive Poisson's ratio ranging between 0 and 0.5. Although a few single crystal materials, e.g., pyrite [1] and cadmium [3], are found to exhibit a negative Poisson's ratio, they are not isotropic. Isotropic material with a negative Poisson's ratio had been veiled in secrecy for many years until 1987 when an auxetic cellular/porous material was produced and tested under compression by Lakes, showing a Poisson's ratio around -0.6 to -0.7 [4]. After that, auxetic behaviour has also been found in different structures. In contrast to the general cognition that negative Poisson's ratio is rare in crystalline solids, 69% of cubic elemental metals exhibit auxetic behaviour when stretched along the [1 1 0] direction [5]. Several idealized zeolites and molecular structures are found to possess a negative Poisson's ratio, and have been explained by their geometry and deformation mechanisms [6, 7]. Silicon dioxide (SiO_2) in the α-cristobalite structure exhibits a negative Poisson's ratio averaging around -0.16 [8]. Negative Poisson's ratio behaviour is also found in the deformation experiments of natural layered ceramic [9], single- or multi-layered graphene [10], 2D puckered structure of $PdSe_2$ monolayer [11], and nanolayered graphene/Cu composites [12]. Very large Poisson's ratio (from -5 to -11) has been observed in the thorough-thickness direction in highly porous fibre networks made of 316L fibres [13]. However, all the aforementioned materials are either cellular/porous or highly anisotropic materials.

Poisson's ratio has attracted more and more attention in recent years. With the advance in materials syntheses, experimental measurements and computational simulations, it has been recognised that Poisson's ratio is related to the densification, connectivity, ductility and the toughness of solid materials [14]. It has also been found that the elastic properties of a composite material can be largely affected, thus tuned by the Poisson ratios of the constituent materials [15–17]. Cellular materials are often used as filler in sandwich structures. Compared

to the conventional foam fillers, auxetic materials with a negative Poisson's ratio can enhance the stiffness [15,16], indentation resistance [18,19], crashworthiness, energy absorption performance [20–22], and fracture toughness [23] of sandwich structures.

The research of negative Poisson's ratio materials was initially supported by NASA/Boeing for aviation and aerospace applications [24,25]. Further investigation into the auxetic behaviour proves that many features of negative Poisson's ratio materials are desirable in aerospace industry [26,27]. Conventional honeycombs [28,29] and open-cell foams [30], which have a positive Poisson's ratio under small deformation, can also exhibit a negative Poisson's ratio (i.e., auxetic behaviour) under large strain compression due to the cell junction/vertex rotation. Most fabricated materials with a negative Poisson's ratio are porous in macro or micro scale, with relatively low stiffness, which may limit their applications to low load-bearing structures. When high stiffness/weight ratio, high strength and energy absorption are all demanded, solid composite materials may be a good choice. Compared to the conventional particle reinforced and unidirectional fibre reinforced composites [31–34], interpenetrating phase composites (IPCs) reinforced by a self-connected network rather than by separated particles or fibres, have been demonstrated to have much better mechanical and physical properties [16, 17, 35–38] than those of their conventional counterparts. When a self-connected auxetic lattice structure or fibre-network is embedded as reinforcement in a matrix with a low positive Poisson's ratio, the composite would have the potential to exhibit auxetic behaviour. It has already been experimentally demonstrated that composite plates reinforced by an auxetic fibre-network exhibits a negative Poisson's ratio in the thickness direction [39]. Composites reinforced by a re-entrant hexagonal honeycomb are also found to exhibit strong in-plane auxetic behaviour [40]. Available publications on composites with auxetic behaviour are very limited and the properties are in general anisotropic. In this paper, we study the mechanical behaviour of solid interpenetrating composites reinforced by three different types of auxetic fibre-networks with cubic symmetry. The concavity of the fibre-networks is considered as a key factor affecting

the auxetic behaviour of the constructed composites. The effects of the volume fraction, elastic properties and concavity of the fibres, and the structural hierarchy on the elastic properties of the interpenetrating auxetic composites are investigated by computational simulation.

2. Geometric structures and computational methods

2.1 Geometric structures

Re-entrant foams are the most common auxetic cellular-network materials, examples include 2D re-entrant honeycombs [18,40], 3D re-entrant foams [4], double-arrowhead re-entrant structure [41], star-shaped structure [42]. In this paper, we study the elastic properties of interpenetrating composites which are reinforced by three different types of regular re-entrant fibre-networks. As all the three types of interpenetrating composites are periodic and have cubic symmetry, we use representative volume elements (RVEs) to study their elastic properties. The RVE of the type I re-entrant fibre-network, as shown in Fig. 1 (a), has 12 self-connected chevron struts in its 6 rectangular diagonal planes, each of which contains two chevron struts. The RVE of the type II re-entrant fibre-network is shown in Fig. 1 (b), which consists of 6 self-connected inward crosses. The RVE of the type III re-entrant fibre-network is shown in Fig. 1(c), which is similar to structure in [42].

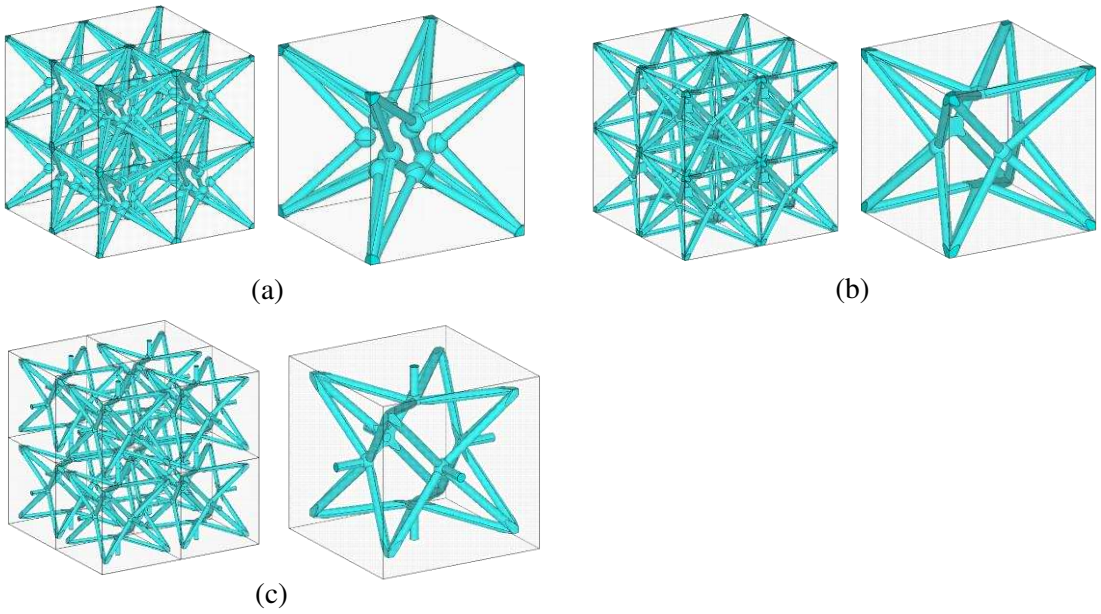

Fig. 1. The geometric structures of the three different types of self-connected reinforcement auxetic fibre-networks: (a) Type I, (b) Type II, (c) Type III.

2.2 Model parameters

One of the most important parameters for a two-phase interpenetrating composite is the fibre volume fraction. For the three different types of re-entrant fibre-networks, all the fibres are assumed to have the same uniform circular cross-section. The fibre volume fraction V_f can be controlled by varying the fibre diameter or the fibre direction angle α shown in Fig. 2. Because of the natural limit of the fibre-network geometric structures, the fibre volume fraction V_f considered in this paper is limited in the range from 4% to 32% for type I and II composites, and from 2.5% to 20% for type III composites. For the three types of interpenetrating composites, their negative Poisson's ratio and other elastic properties (e.g., Young's modulus) significantly depend on the chevron or the re-entrant angle α. In order to explore how the fibre angle affects the elastic properties of the three types of interpenetrating composites, the following three sets of angles given in table 1 are used in simulations.

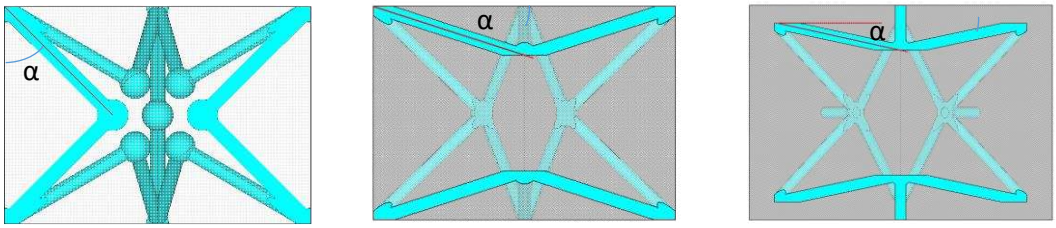

(a) (b) (c)

Fig. 2. Fibre direction angle α in the three different types of reinforcement fibre-networks. (a) the chevron angle α measured in the main diagonal plane of the type-I RVE; (b) and (c) the re-entrant angle α measured in the RVE main diagonal plane of the type I and II composites.

Table 1. Fibre angle α of the three different types of reinforcement fibre-networks.

	Angle 1	Angle 2	Angle 3	Angle 4
Type I	20°	30°	40°	
Type II	10°	12°	14°	20°
Type III	12°	20°	24°	26°

It is assumed that the reinforcement fibre-network and the matrix of the interpenetrating composites are made by two different isotropic solid materials. Their Young's moduli and Poisson's ratios are denoted as E_f, E_m, ν_f, ν_m, where subscript f stands for fibre and m represents matrix. For simplicity and generality, both the Young's moduli of the fibre and the matrix are normalised by that of the matrix, thus the normalised Young's modulus of the matrix is always 1 and the possible range of the normalised Young's modulus of the fibre is given in Table 2. The range of the Young's moduli is from 60 to 400 GPa for most metal, alloys, ceramics and carbon fibres; and from 0.1 to 10 GPa for most solid polymers [43]. For example, low density Polyethylene has a Young's modulus of 0.15 – 0.24 GPa [43]. In some 3D printed composites [44], VeroWhite (rigid photopolymer) is often used as the stiffer phase whose Young's modulus is $E_f = 1.66\text{GPa}$, and TangoPlus (a soft rubbery material) is often used as

the softer phase whose Young's modulus is $E_m = 0.7456\text{MPa}$. Thus, the ratio E_f/E_m in such composites is close to 2500. In most polymer, rubber or metal matrix composites reinforced by a metal or ceramic, the ratio E_f/E_m stays in the range from 2 to 1000, examples include ceramics/steel composites, Al/epoxy composites [45], glass/epoxy composites [46] and Al/Al_2O_3 composites [47]. In order to enhance the auxetic behaviour (i.e., a large negative Poisson's ratio), a relatively high value of E_f/E_m is desired.

Table 2. The range of the normalised Young's Moduli of the fibre material.

E_f/E_m	2	10	50	100	500	1000	2000

The elastic properties of composites can be significantly affected by the Poisson's ratio of the matrix material [15-17], but are less sensitive to that of the reinforcement material (this may be because the volume fraction of the latter is usually much smaller). As almost all the single-phase solid isotropic materials have a positive Poisson's ratio, a very small Poisson's ratio is desired for the matrix material in order to enhance the auxetic behaviour of the composites. For the aforementioned materials as the potential reinforcement and matrix phases, the Poisson's ratios of TangoPlus and VeroWhite are approximately 0.49 and 0.3 [44,48]. Aluminium has a Poisson's ratios around 0.33. Their Poisson's ratios are too large for isotropic auxetic IPCs to exhibit a significant negative Poisson's ratio. Carbon matrix can have a very low Poisson's ratio from approximately 0 to 0.05 [49], and the Poisson's ratio of SiC matrix is around 0.14 to 0.35. In metal matrix composites, beryllium which is used as the matrix material in AlBeMet for aerospace and commercial applications has a very low Poisson's ratio of 0.03 [50]. Table 3 gives the Poisson's ratios of the possible isotropic solid matrix and fibre materials discussed in this paper.

Table. 3. Poisson's ratios of the fibre and matrix materials.

υ_f	0.35	0.25	
υ_m	0	0.1	0.2

2.3 Computational method

The representative volume element (RVE) models of the composites reinforced by the three different types of auxetic fibre-networks are constructed using the ANSYS software [51]. As each of the three types of composites is made of a large number of identical representative volume elements (RVEs), their elastic properties can be obtained from single RVE models. Both the fibre and matrix materials are assumed to be homogeneous and isotropic solids, and they both are partitioned into higher order 3D, 10-node tetrahedra (Solid187) elements. As all the three types of composites are periodic, periodic boundary conditions are applied to the RVE models in the finite element simulations [15,16]. To obtain the Young's modulus and Poisson's ratios, a small tensile strain of 0.1% is applied to the RVE models in all the simulations.

3. Results

The focus of this study is on their function side, e.g., the negative or zero Poisson's ratios. As all the three types of composites have cubic symmetry in their geometric structure, they have only three independent elastic constants and their elastic properties are nearly isotropic, e.g., their Poisson's ratios are the same in their three orthogonal symmetric planes.

3.1 Effects of fibre volume fraction on the Poisson's ratio of the composites

The Poisson's ratios of the three different types of composites strongly depend on the fibre volume fraction. When the fibre angle is fixed at $\alpha = 20°$ for all the three different types of composites (see Fig. 2), Fig. 3(a) shows the dependencies of their Poisson's ratios on the fibre volume fraction while other parameters are fixed at $\nu_m = 0.1,\ \nu_f = 0.25,\ E_f/E_m = 1000$; and Fig. 3 (b) presents the similar relationships when $\nu_m = 0,\ \nu_f = 0.25,\ E_f/E_m = 1000$.

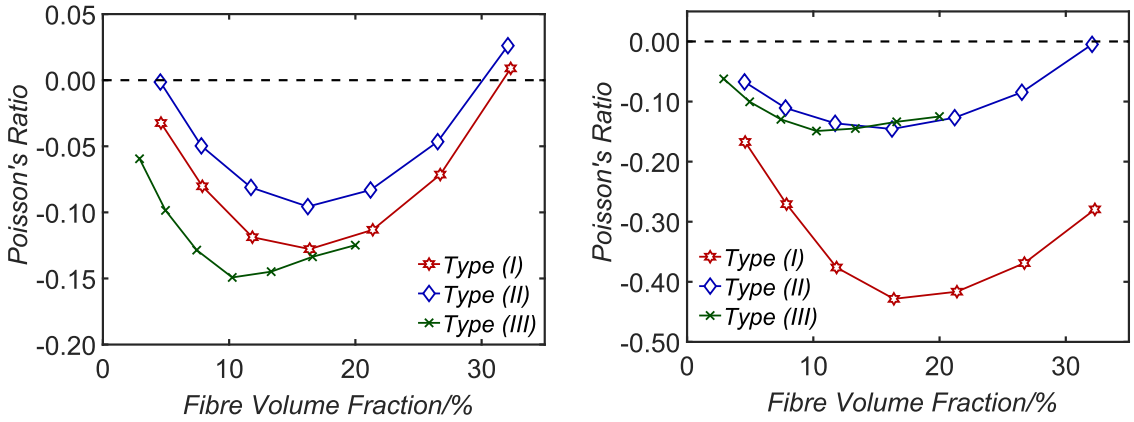

Fig. 3. Effects of fibre volume fraction on the Poisson's ratio of the composites when $\alpha = 20°$. (a) $\nu_m = 0.1, \nu_f = 0.25,\ E_f/E_m = 1000$; (b) $\nu_m = 0, \nu_f = 0.25,\ E_f/E_m = 1000$.

As can be seen in Fig.3, all the three different types of composites exhibit a very strong negative Poisson's ratio when the fibre volume fraction is in range from 2.5% to 30%. The focus of this research is on the negative Poisson's ratio (i.e., the auxetic behaviour). Outside this fibre volume fraction range, the composites may not exhibit a negative Poisson's ratio. Obviously, all the three different types of solid composites could be designed to have a 'zero' Poisson's ratio. Comparison between the results in Fig. 3(a) and Fig. 3(b) illustrates that the Poisson's ratio of the matrix material can strongly affect the auxetic behaviour (i.e., the negative Poisson's ratio) of the composites, the smaller the Poisson's ratio of the matrix material, the larger the magnitude of the negative Poisson's ratio of the composites.

3.2 Effects of fibre angle α on the Poisson's ratios of the composites

Fig. 4 shows the effects of the fibre angle α on the relationships between the Poisson's ratio and the fibre volume fraction of the three different types of composites when all the other parameters are fixed at $\nu_m = 0.1,\ \nu_f = 0.25,\ and\ E_f/E_m = 1000$. As can be seen, the fibre angle can strongly affect the Poisson's ratios of the composites. In order to achieve large magnitude of negative Poisson's ratio for the composites, a suitable (or an optimal) fibre angle α is critical. This is consistent with the experimentally measured results in anisotropic composite [40] which showed that it is possible to obtain different magnitudes of negative Poisson's ratios by changing the cell wall angle θ of the reinforcement re-entrant honeycomb.

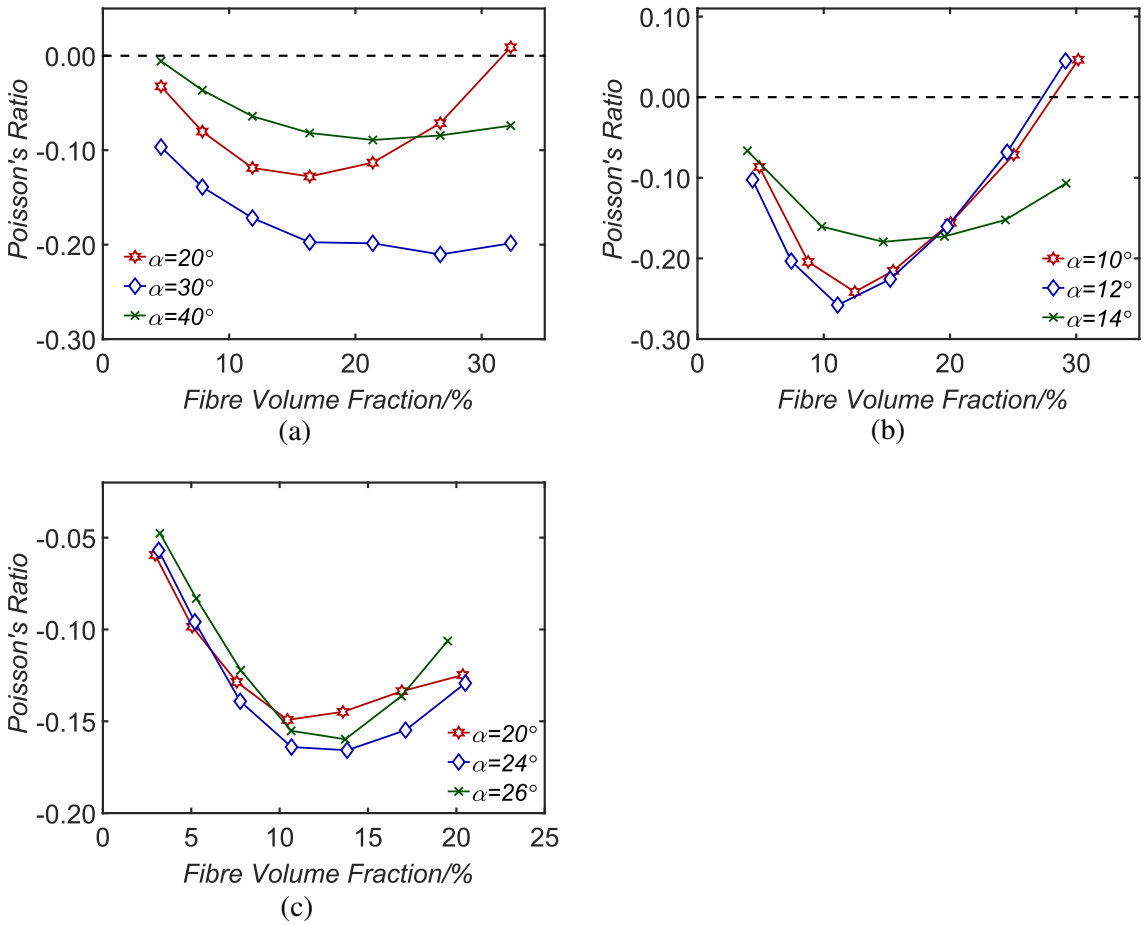

Fig. 4. Effects of the fibre angle α on the relationships between the Poisson's ratio and the fibre volume fraction of the three different types of composites. (a) Type I; (b) Type II; (c) Type III.

Figure 4 (a) shows clearly that the magnitude of the negative Poisson's ratio of the type-I composites with $\alpha = 30°$ is much larger than those of the same type composites with $\alpha = 20°$ and $40°$. Thus, it is certain that there exists a fibre angle between $\alpha = 20°$ and $40°$ for the type I composites, which enables the optimal (maximum) auxetic behaviour. Figure 4 (b) illustrates that the Type II composites with a fibre angle of $\alpha = 12^0$ has a larger magnitude of negative Poisson's ratios than the cases when $\alpha = 10^0$, 14^0 and 20^0 (see Fig. 3(a)), logically, the maximum (optimal) auxetic behaviour of the type II must exist when the fibre angle is close to 12^0. Similarly, Figure 4 (c) demonstrates that the magnitude of the negative Poisson's ratio of the type-I composites with $\alpha = 24°$ is much larger than those the same type composites with $\alpha = 20°$ and $26°$. For all the three different types of composites, their negative Poisson's ration are resulted from their self-connected fibre-networks whose auxetic (i.e., negative Poisson's ratio) behaviours have to overcome the effects of the positive Poisson's ratio of the matrix material. Thus, the different optimal fibre angles of the type II and type III composites depend on their geometrical structures and the interplay between their auxetic fibre-network and matrix materials.

3.3 Effects of E_f/E_m on the Poisson's ratio of the composites

When $\alpha = 20°$, $\nu_m = 0.1$ and $\nu_f = 0.25$, the effects of E_f/E_m on the relationship between the Poisson's ratio and the fibre volume fraction of the type III composites are illustrated in Fig. 5. As can be seen, the larger the ratio of E_f/E_m, the more obvious auxetic behaviour the composites exhibit. With the reduction of E_f/E_m, the auxetic behaviour of the composites gradually disappears. This is because the self-connected auxetic fibre-network with a larger value of E_f/E_m can more strongly dominate the auxetic behaviour of the composites. If $E_f/E_m = 1$, the Poisson's ratio of the composites would be approximately $V_m\nu_m + V_f\nu_m$ and be independent of the geometrical structure of the fibre network, where V_m and V_f are the volume fractions of the fibre-network and the matrix, respectively.

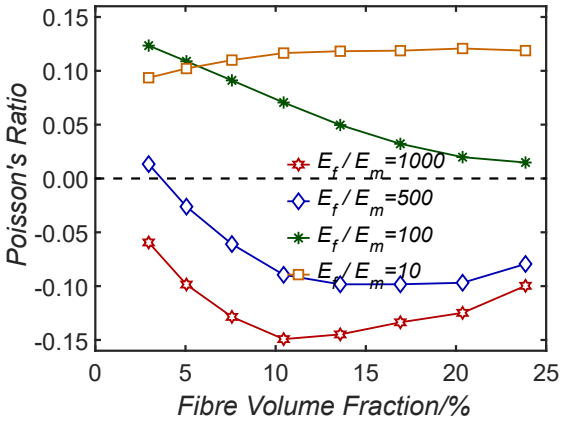

Fig. 5. Effects of E_f/E_m on the relationship between the Poisson's ratio and the fibre volume fraction of the type III composites with $\nu_m = 0.1$, $\nu_f = 0.25$, and fibre angle $\alpha = 20°$.

3.4 Effects of E_f/E_m on the relationship between the Young's modulus and the fibre volume fraction of the composites

Although the focus of the study is on the auxetic behaviour (i.e., negative Poisson's ratio) of the solid composites, the stiffness is a very important property to enable the desired functions in applications. When the fibre angle is fixed at $\alpha = 20°$, Fig. 6 shows the effects of the ratio E_f/E_m on the relationship between the Young's modulus and the fibre volume fraction of the type I composites with $\nu_m = 0.1$, $\nu_f = 0.25$. It is noted that the Young's moduli of the composites have been normalised by that of the matrix material. As can be seen, the larger the ratio E_f/E_m, the larger the Young's modulus of the composites.

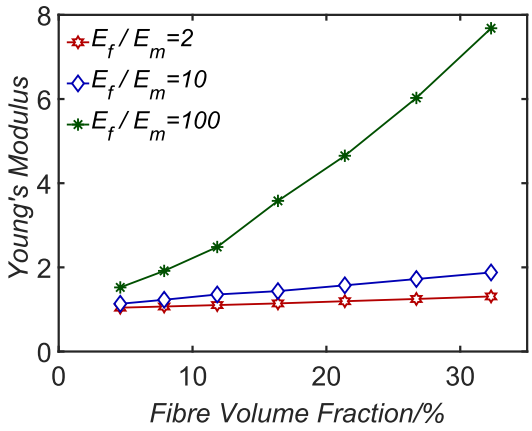

Fig. 6. Effects of E_f/E_m on the relationship between the Young's modulus and the fibre volume fraction of the type I composites with $\nu_m = 0.1$, $\nu_f = 0.25$.

4. Discussion

Negative Poisson's ratio has important applications and extensive research works have been done on the auxetic behaviour/properties of cellular/porous materials [4,6] and anisotropic materials [3,5,7,9,12,13]. Although cellular/porous materials [4,6] can be designed to have a large magnitude negative Poisson's ratio, they are obviously much weaker and softer compared to their counterpart solid or composite materials without any pore. Some single crystal materials [4,7,8], single- or multi-layered graphene [10], and 2D puckered structure of $PdSe_2$ monolayer [11], and nanolayered graphene/Cu composites [12] also exhibit the auxetic behaviour, however, their properties are anisotropic. Moreover, it is very expensive and very difficult to produce a large bulk of such materials for practical applications.

All the three different types of composites studied in this paper do not contain any pore and their elastic properties are almost isotropic. Because of their negative Poisson's ratio behaviour, the unique indentation response of these auxetic composite makes them ideal materials for impact resistance applications [6] such as helmet and body armour [54]. As the Poisson's ratio of those composites can be tuned to zero or any-value near zero, they can be used in biomedical applications to imitate the Poisson's ratio of bones, tissue or joints of human body [55], or used to produce micro-sized robot to clean the vein in human body because they can reduce the lateral expansion under the thrust/drag force [6, 56]. To enable the desired auxetic function in

applications, the composites should have a sufficiently large stiffness. Here we compare the Young's moduli of the three different types of auxetic composites with the experimentally measured Young's moduli of their conventional counterpart isotropic particle composites [46,52,53]. Table 4 gives the elastic properties of the constituent materials of these conventional particle composites.

Table 4. The elastic properties of the constituent materials in particle composites.

Composites	E_f (MPa)	ν_f	E_m (MPa)	ν_m
SiC /Al [52]	410000	0.19	74000	0.33
Glass/Polystyrene [53]	70000	0.22	3250	0.34
Glass /Epoxy [46]	69000	0.15	3000	0.35

In order to compare the Young's moduli of the auxetic interpenetrating composites with those of the conventional particle composites, the component properties E_f, E_m, ν_f, ν_m and the fibre volume fractions of the three different types of auxetic interpenetrating composites are chosen to be same as those given in table 4. Fig. 7 shows the comparison between the Young's moduli of the three different types of auxetic interpenetrating composites and those of the conventional particle composites, where the Young's moduli of the composites are normalised by the Voigt limit (i.e., $E_f V_f + E_m V_m$), V_f and V_m are the volume fractions of the fibre (or particle in literature) and the matrix, respectively. The fibre angles of the three types of auxetic composites are chosen as $\alpha = 20°$ for type I, and $\alpha = 12°$ for types II and III.

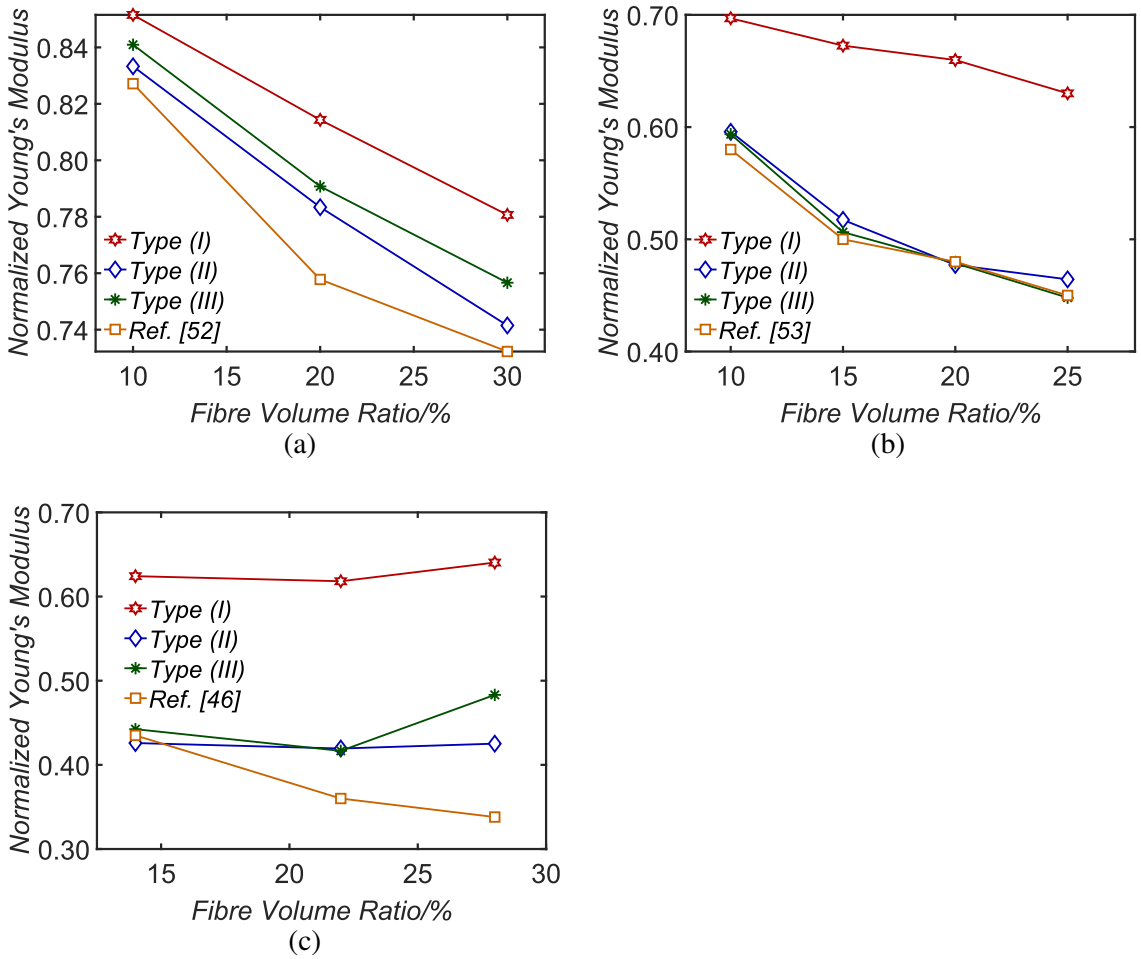

Fig. 7. Comparison between the normalized Young's moduli of auxetic interpenetrating composites and those of the conventional particle composites: (a) with the SiC/Al particle composites [52], (b) with the glass/polystyrene particle composites [53], and (c) with the glass /epoxy particle composite [46].

As can be seen in Fig. 7, the Young's moduli of all the three different types of auxetic interpenetrating composites are clearly larger than those of the conventional particle composites [46, 52, 53], and the type I interpenetrating composites obviously have the largest Young's moduli among the three different types of auxetic composites. Thus, the three types of composites can be used not only as functional materials (with negative Poisson's ratio), but also as structural materials (with high stiffness). It is noted that the stiffness of auxetic composites is usually smaller than that of non-auxetic interpenetrating composites. For example, the interpenetrating composites reinforced by a self-connected fibre network with a

cubic lattice structure [16] which could have an almost isotropic Young's modulus much larger than the Voight limit. Moreover, composites [15] reinforced by a perfect regular closed-cell foam with identical cubic cells of a uniform wall thickness are almost isotropic, and have the largest Young's modulus compared to any other type of isotropic composites.

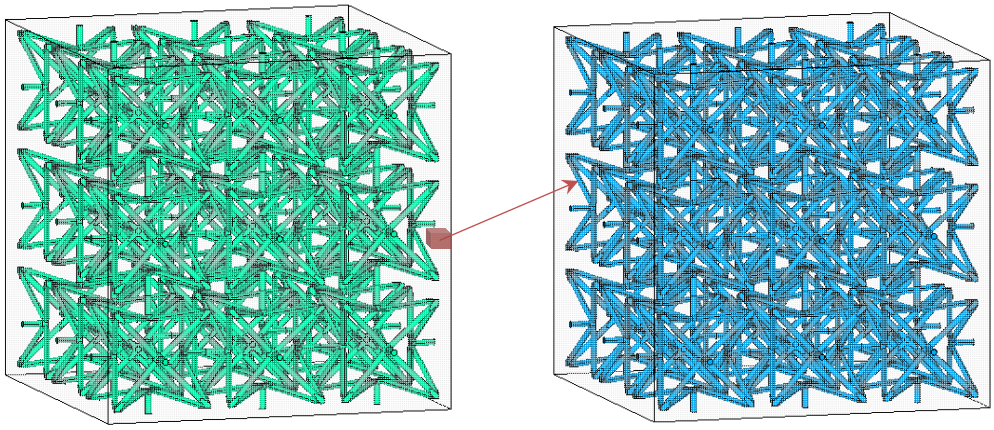

(a) Level-2 composite (b) Level-1 Composite

Fig 8. Illustration of the type-III hierarchical and self-similar composite in which the 'matrix' of the level-2 composite (a) is the level-1 composite (b).

Structural hierarchy has been demonstrated to be able to significantly enhance the mechanical properties of composites [15,16]. Here, the three types of interpenetrating composites are assumed to be hierarchical and self-similar with a few levels of structural hierarchy, and the 'matrix' in a higher-level composite is made of the similar lower-level composite, as illustrated in Fig. 8. The Young's modulus and Poisson's ratio of the three types of level-1 composites, in which the matrix is a single-phase solid material, are already obtained as illustrated in Figures 3-7. To demonstrate the effects of structural hierarchy, we use the type III hierarchical and self-similar composites with a fixed fibre angle of $\alpha = 20°$ as example. The level-1 composite is made of two different single-phase solids, and their elastic properties are $E_f/E_m = 1000$, $\nu_m = 0.1$ and $\nu_f = 0.25$. For the level-2 composites, the main strengthening

fibre network is made of the same solid material (i.e., $E_f/E_m = 1000$ and $\nu_f = 0.25$) and the 'matrix' is made of the self-similar level-1 composite whose Young's modulus and Poisson's ratio are obtained by FEM simulation. Thus, the Poisson's ratio of the level-2 and level-3 hierarchical and self-similar type III composites can be obtained as shown in Fig. 9. As can be seen, structural hierarchy can significantly enhance the auxetic behaviour of the composites and their negative Poisson's ratio could reach a large magnitude.

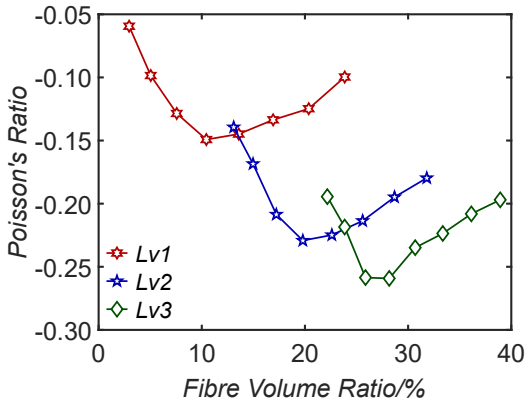

Fig. 9. The relationship between the Poisson's ratio and the fibre volume fraction of hierarchical and self-similar type III composites with a fixed fibre angle of $\alpha = 20°$.

5. Conclusion

Most materials with a negative Poisson's ratio are either cellular/porous materials or highly anisotropic materials. Solid interpenetrating composites reinforced by three different types of auxetic fibre-networks are studied in this paper. They all could have either a positive, or a negative, or a zero Poisson's ratio. The magnitude of the Poisson's ratio depends on the combination between the fibre angle α, the structural type of the fibre-network, the fibre volume fraction, and the mechanical properties of the component materials: E_f/E_m, ν_f and ν_m. As the composites do not contain any pore in structure and the strengthening phase is a self-connected network, the Young's moduli of the three types of composites are obviously larger

than those of the conventional particle composites. In addition, as all the three types of composites have cubic symmetry, their mechanical properties are almost isotropic. Moreover, structural hierarchy can significantly enhance the auxetic behaviour of the composites. Therefore, the three different types of auxetic interpenetrating composites could be used not only as functional materials, but also as structural materials in engineering applications.

Acknowledgments

Zhengyang Zhang is grateful for the support of School of Engineering, Cardiff University and China Scholarship Council.

References

[1] Love AEH. A treatise on the mathematical theory of elasticity. Cambridge university press; 2013.

[2] L.D. Landau and E.M. Lifshitz. Theory Of Elasticity. vol. 7. 1970.

[3] Li Y. The anisotropic behavior of Poisson's ratio, Young's modulus, and shear modulus in hexagonal materials. Phys Status Solidi 1976;38:171–5.

[4] Lakes Roderic. Foam Structures with a Negative Poisson ' s Ratio. Science (80-) 1987;235:1038–40.

[5] Baughman RH, Shacklette JM, Zakhidov AA, Stafstrom S. Negative Poisson's ratios as a common feature of cubic metals. Nature 1998;392:362–5.

[6] Evans KE, Alderson A. Auxetic materials: Functional materials and structures from lateral thinking! Adv Mater 2000;12:617–28.

[7] Grima JN, Jackson R, Alderson A, Evans KE. Do Zeolites Have Negative Poisson's Ratios? Adv Mater 2000;12:1912–8.

[8] Yeganeh-haeri A, Weidner DJ, Parise JB. A Silicon Dioxide with a Elasticity of α-Cristobalite : Negative Poisson ' s Ratio. Science (80-) 1992;257:650–2.

[9] Song F, Zhou J, Xu X, Xu Y, Bai Y. Effect of a negative poisson ratio in the tension of ceramics. Phys Rev Lett 2008;100:1–4.

[10] Hou J, Deng B, Zhu H, Lan Y, Shi Y, De S, Liu L, Chakraborty P, Gao F, Peng Q, Magic auxeticity angle of graphene, Carbon 2019;149: 350-354.

[11] Liu G, Zeng Q, Zhu P, Quhe R, Lu P. Negative Poisson's ratio in monolayer PdSe2. Comput Mater Sci 2019;160:309–14.

[12] Zhang C, Lu C, Pei L, Li J, Wang R, Tieu K. The negative Poisson's ratio and strengthening mechanism of nanolayered graphene/Cu composites. Carbon 2018;143:125–37.

[13] Neelakantan S, Bosbach W, Woodhouse J, Markaki AE. Characterization and deformation response of orthotropic fibre networks with auxetic out-of-plane behaviour. Acta Mater 2014;66:326–39.

[14] Greaves GN, Greer AL, Lakes RS, Rouxel T. Poisson's ratio and modern materials. Nat Mater 2011;10:823–37.

[15] Zhu H, Fan T, Zhang D. Composite materials with enhanced dimensionless Young's modulus and desired Poisson's ratio. Sci Rep 2015;5:14103.

[16] Zhu H, Fan T, Xu C, Zhang D. Nano-structured interpenetrating composites with enhanced Young's modulus and desired Poisson's ratio. Compos Part A Appl Sci Manuf 2016;91:195–202.

[17] Lin X, Zhu HX, Yuan X, Wang Z, Bordas S, The elastic properties of composites reinforced by a transversely isotropic random fibre-network, Composite Structures, 2019;208:33-44.

[18] Lakes RS, Elms K. Indentability of Conventional and Negative Poisson's Ratio Foams. J Compos Mater 1993;27:1193–202.

[19] Hu LL, Zhou MZ, Deng H. Dynamic indentation of auxetic and non-auxetic honeycombs under large deformation. Compos Struct 2019;207:323–30.

[20] Liu W, Huang J, Deng X, Lin Z, Zhang L. Crashworthiness analysis of cylindrical tubes filled with conventional and negative Poisson's ratio foams. Thin-Walled Struct 2018;131:297–308.

[21] Lethbridge ZAD, Williams JJ, Walton RI, Smith CW, Hooper RM, Evans KE. Direct, static measurement of single-crystal Young's moduli of the zeolite natrolite: Comparison with dynamic studies and simulations. Acta Mater 2006;54:2533–45.

[22] Gao Q, Zhao X, Wang C, Wang L, Ma Z. Multi-objective crashworthiness optimization for an auxetic cylindrical structure under axial impact loading. Mater Des 2018;143:120–30.

[23] Choi JB, Lakes RS. Fracture toughness of re-entrant foam materials with a negative Poisson's ratio: Experiment and analysis. Int J Fract 1996;80:73–83.

[24] Lakes RS. Design considerations for materials with negative Poisson's ratios. J Mech Des 1993;115:696–700.

[25] Lakes R. Deformation mechanisms in negative Poisson's ratio materials: structural aspects. J Mater Sci 1991;26:2287–92.

[26] Alderson A, Alderson KL. Auxetic materials. Proc Inst Mech Eng Part G J Aerosp Eng 2007;221:565–75.

[27] Liu Q. Literature Review: Materials with Negative Poisson's Ratios and Potential Applications to Aerospace and Defence. 2006.

[28] Zhu HX, Mills NJ. The in-plane non-linear compression of regular honeycombs. Int J Solids Struct 2000;37:1931–49.

[29] Zhu HX, Thorpe SM, Windle AH. The effect of cell irregularity on the high strain compression of 2D Voronoi honeycombs. Int J Solids Struct 2006;43:1061–78.

[30] Zhu HX, Windle AH. Effects of Cell Irregularity on the High Strain Compression of Open-Cell Foams. Acta Mater 2002;50:1041–52.

[31] Rawal S. Metal-matrix composites for space applications. Jom 2001;53:14–7.

[32] Kumar GBV, Rao CSP, Selvaraj N. Mechanical and Tribological Behavior of Particulate Reinforced Aluminum Metal Matrix Composites – a review. J Miner Mater Charact Eng 2011;10:59–91.

[33] Sadeghian Z, Lotfi B, Enayati MH, Beiss P. Microstructural and mechanical evaluation of Al-TiB2 nanostructured composite fabricated by mechanical alloying. J Alloys Compd 2011;509:7758–63.

[34] Zhang Q, Xu X, Lin D, Chen W, Xiong G, Yu Y, et al. Hyperbolically Patterned 3D Graphene Metamaterial with Negative Poisson's Ratio and Superelasticity. Adv Mater 2016;28:2229–37.

[35] Clarke DR. Interpenetrating Phase Composites. J Am Ceram Soc 1992;75:739–58.

[36] Peng HX, Fan Z, Evans JRG. Bi-continuous metal matrix composites. Mater Sci Eng A 2001;303:37–45.

[37] Moon RJ, Tilbrook M, Hoffman M, Neubrand A. Al-Al 2O 3 composites with interpenetrating network structures: Composite modulus estimation. J Am Ceram Soc 2005;88:666–74.

[38] Huang LJ, Geng L, Peng HX, Balasubramaniam K, Wang GS. Effects of sintering parameters on the microstructure and tensile properties of in situ TiBw/Ti6Al4V composites with a novel network architecture. Mater Des 2011;32:3347–53.

[39] Jayanty S, Crowe J, Berhan L. Auxetic fibre networks and their composites. Phys Status Solidi Basic Res 2011;248:73–81.

[40] Subramani P, Rana S, Ghiassi B, Fangueiro R, Oliveira D V., Lourenco PB, et al. Development and characterization of novel auxetic structures based on re-entrant hexagon design produced from braided composites. Compos Part B Eng 2016;93:132–42.

[41] Larsen UD, Sigmund O, Bouwstra S. Design and fabrication of compliant micromechanisms and structures with negative Poisson's ratio. J Microelectromechanical Syst 1997;6:99–106.

[42] Zhu H, Fan T, Peng Q, Zhang D, Giant thermal expansion in 2D and 3D cellular

materials, Advanced Materials 2008;30:1705048.

[43] Gibson LJ, Ashby MF, Cellular Solids, Pergamon Press, 1988.

[44] Al-Ketan O, Al-Rub RKA, Rowshan R. Mechanical Properties of a New Type of Architected Interpenetrating Phase Composite Materials. Adv Mater Technol 2017;2:1600235.

[45] Jhaver R, Tippur H. Processing, compression response and finite element modeling of syntactic foam based interpenetrating phase composite (IPC). Mater Sci Eng A 2009;499:507–17.

[46] Rousseau C-E, Tippur H. Compositionally graded materials with cracks normal to the elastic gradient. Acta Mater 2000;48:4021–33.

[47] Breslin MC, Ringnalda J, X L, Fuller M, Seeger J, Daehn GS, et al. Processing , microstructure , and properties of co-continuous alumina- aluminum composites. Mater Sci Eng A 1995;195:113–9.

[48] Li T, Chen Y, Hu X, Li Y, Wang L. Exploiting negative Poisson's ratio to design 3D-printed composites with enhanced mechanical properties. Mater Des 2018;142:247–58.

[49] Li X, Zhang Z, Qin L, Yang X, Feng Z, Wang Y, et al. Measuring Mechanical Properties of the 3D Carbon/Carbon Composite Using Automated Grid Method. J Test Eval 2013;41:20120006.

[50] Parsonage T. Beryllium metal matrix composites for aerospace and commercial applications. Mater Sci Technol 2013;16:732–8.

[51] *ANSYS® Academic Research Mechanical, Release 16.0.*

[52] Chawla N, Sidhu RS, Ganesh V V. Three-dimensional visualization and microstructure-based modeling of deformation in particle-reinforced composites. Acta Mater 2006;54:1541–8.

[53] Dekkers MEJ, Heikens D. The effect of interfacial adhesion on the tensile behavior of polystyrene–glass-bead composite.pdf. J Appl Polym Sci 1983;28:3809–15.

[54] M. Sanami, N. Ravirala, K. Alderson, A. Alderson, Auxetic materials for sports applications, Procedia Engineering. 72 (2014) 453–458.

[55] G.E. Stavroulakis, Auxetic behaviour: Appearance and engineering applications, Physica Status Solidi (B) Basic Research. 242 (2005) 710–720.

[56] K.E. Evans, K.L. Alderson, Auxetic materials : the positive side of being negative, (2000).